Modular Modeling and Statistical Validation for Grid-Connected FS-MPC-Controlled Matrix Converters

Novak, Mateja; Grobelna, Iwona; Nyman, Ulrik Mathias; Szcześniak, Paweł; Blaabjerg, Frede

Published in:
IEEE Transactions on Industrial Electronics

DOI (link to publication from Publisher):
10.1109/TIE.2022.3206699

Publication date:
2023

Document Version
Accepted author manuscript, peer reviewed version

Modular Modelling and Statistical Validation for Grid Connected FS-MPC Controlled Matrix Converters

M. Novak, *Member, IEEE*, I. Grobelna, *Member, IEEE*, U. Nyman,
P. Szczesniak, *Senior Member, IEEE*, and F. Blaabjerg, *Fellow Member, IEEE*

***Abstract*—In recent publications statistical model checking (SMC) has been proposed as a method for verifying the performance of finite-set model predictive control (FS-MPC) algorithms applied to power electronics converters. One of the reasons the full potential of the method in the power electronics systems (PES) has not yet been explored is the time consuming modelling process. In this paper we propose a modular method of modelling the power electronics system components by providing simple building blocks, which can be connected to build different PES. The modelling method is here demonstrated on a direct matrix converter, which operates in a stochastic grid with different harmonic distortion levels and voltage sags. By applying the SMC, the performance of the control algorithm in terms of the output current distortion, effects of the weighting factor selection and grid distortions on the device utilization can be evaluated. The obtained results confirm, that high grid distortions and voltage sags will increase the stress of several devices. This information can be of great importance to identify the most stressed components and how the control algorithm can be adapted to extend the lifetime of the components and thereby the system during different grid conditions. The verified FS-MPC algorithm has also been implemented in an experimental set-up.**

***Index Terms*—finite-set model predictive control, hybrid automata, modelling, performance verification, power converter, statistical model checking.**

I. Introduction

THE model predictive control algorithm has established its place as a promising alternative to conventional control algorithms in power electronics systems (PES) [1], [2]. Due to the versatility of the control algorithm it has been employed in multiple power electronics converter topologies and applications [3]. For every control algorithm, performance verification plays a key role before commissioning of the converter system [4]. One of the goals of the control algorithm verification is to evaluate how disturbances and algorithm parameters affect the performance metrics of the PES, such as reference tracking or robustness with respect to parameter variations. On the other hand, with respect to reliability, the goal of verification could be to check how disturbances or algorithm parameters affect the device stress distribution, e.g., which devices are the most stressed thermally and under which conditions.

The conventional methods for verifying the control algorithm performance in PES [4] are by simulations and experiments. Formal verification methods, among which the most valuable are symbolic model checking and statistical model checking (SMC), are so far rarely used in the PES despite their wide success in the other domains. In general, formal methods allow the identification of some divergences between the formal model of the system and the requirements. Symbolic model checking [5] gives results with 100% confidence, but cannot be directly applied in some areas, especially for large systems with stochastic components. It can be used to check the structural properties of the control algorithm, verifying whether all states of the controller are reachable as shown in [6] for a matrix converter and in [7]–[9] for dc-dc converters. The method can be used to compare the performance of two different types of controllers [10]. There are also different ways of modelling the system, so it is suitable for the model checking application, e.g., the system in [6] has been specified as a Petri net and then formally written as an abstract rule-based logical model and transformed into a verifiable model in the format of a nuXmv model checker. In [7]–[10] the system was modelled using the hybrid automata structures.

The main drawback of symbolic model checking is that it suffers from the state explosion problem (the larger the model, the longer the exploration of the entire model state space). Moreover, once components that do not have a deterministic behaviour, such as loads or power grid, are introduced into the model, it is almost impossible to explore all possible scenarios. In turn, SMC [11], [12], as a combination of simulation and statistical methods, allows gaining of statistically valid results that predict system behaviour with some degree of confidence that is preset by the user (e.g., 0.95 confidence level). The main advantage of SMC is that there is no need for a full state space exploration, hence it does not suffer from a state space explosion problem. SMC uses well-known methods originating from statistics (such as Monte Carlo simulations) to obtain the statistical evidence of the system properties.

Manuscript received November 17, 2021; revised March 17, 2022, June 22, 2022 and August 22, 2022; accepted September 1, 2022. This work was supported in part by the Reliable Power Electronic-Based Power System (REPEPS) project at the AAU Energy, Aalborg University as a part of the Villum Investigator Program funded by the Villum Foundation.

M. Novak and F. Blaabjerg are with AAU Energy, Aalborg University, Aalborg, 9220, Denmark (e-mail: nov@energy.aau.dk, fbl@energy.aau.dk).

I. Grobelna and P. Szczesniak are with Autom. Control, Electronics and Electr. Eng, University of Zielona Góra, Zielona Góra, 65-417, Poland (i.grobelna@iee.uz.zgora.pl, p.szczesniak@iee.uz.zgora.pl).

U. Nyman is with Computer Science Department, Aalborg University, Aalborg, 9220, Denmark (ulrik@cs.aau.dk)

Several toolboxes are available for SMC application. Some of them can be directly applied on Matlab/Simulink models, using plugins of the existing software (e.g., Breach [13], S-TaLiRo [14] or Plasma Lab [15]) or by analysing execution traces collected from the simulations (e.g., with ThEodorE [16]). It is also possible to model the system using timed automaton (TA) (i.e., finite state machine) structures, which are applied to define a timed behaviour and analyse real-time systems [17], e.g., using the UPPAAL SMC toolbox [18]. The focus in this paper will be on advancing the modelling of PES using the hybrid TA structures. They can model all the required dynamics and interactions of PES necessary for control algorithm verification as shown in [19]. As mentioned, there are many SMC toolboxes available.

We have chosen the UPPAAL SMC toolbox for the following reasons:

1) free non-commercial applications in academia;
2) efficiency;
3) intuitiveness and ease of use;
4) direct collaboration with the tool developers.

By creating and simulating a model in UPPAAL SMC and doing the statistical model checking, again in UPPAAL SMC, the best optimization is achieved, since the model is already suitable for a fast SMC application.

While for conventional algorithms used to control the PES, the procedures and methods to verify the above mentioned properties are well developed [20], the model predictive control (MPC) algorithms do not have such powerful methods at their disposal [21]. Thus, when proposing a new control algorithm, designers rely on simulations with parameter sweeps and experiments to verify the algorithm performance and robustness [22]–[24]. However, when using simulations and experiments it is not easy to model the stochastic nature of the load or grid disturbances. Moreover, as the whole state space of a converter cannot be explored, how can the simulations or experimental results be quantified to provide evidence of a system property? In [25] it is shown that statistical tools can be efficiently used for performance evaluation of current control strategies of the power converters and in [19] SMC was used to validate the performance of an MPC algorithm for an UPS system.

Modelling the PES using the TA structures, requires some time investment. While some components of the converter system are easy to be imagined as a type of timed automaton, for some it might take several iterations until the correct behaviour is achieved. In order to speed up this process, in this paper we propose a modular modelling concept of PES using TA. The main advantage of the modular modelling concept is that components of the PES are designed as separate building blocks, where it becomes rather simple to change the converter topology, application, or control algorithm. The building blocks are easy to understand both for electrical and computer science engineers. Moreover, the modelling concept is applicable to other SMC toolboxes with similar features that are based on TA structures. In the long term it will enable building a library of components, where the user will only need to define how the inputs and outputs of the components are interconnected. Furthermore, this also

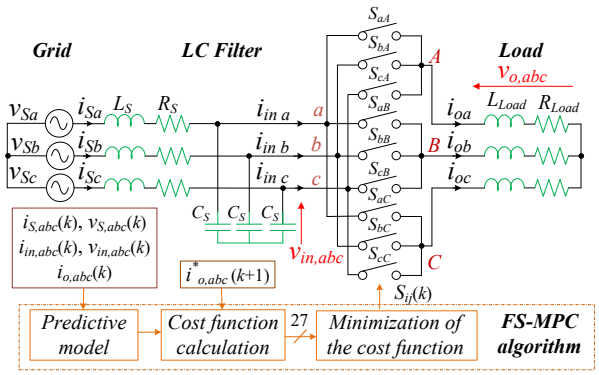

Fig. 1: Simplified scheme of a matrix converter topology using finite set model predictive control algorithm.

offers the possibility of running parallel converters or two different systems in parallel. This was not possible using the modelling approach in [19]. For example, multiple instances of the converter system with different weighting factors can be defined in the same environment (i.e., load or grid conditions). Afterwards, queries that directly compare the performance of these converter systems can be defined.

The modelling concept will be demonstrated on a grid-connected indirect matrix converter as shown in Fig. 1. The FS-MPC (finite-set model predictive control algorithm) has been reported to be a very convenient method for controlling the matrix converter, however due to the lack of performance verification tools it was not possible to complete the comparison to other control methods [24]. The SMC approach applied in this paper can provide the necessary information on how a grid-connected matrix converter performs under different harmonic distortions and voltage sags. In particular, the following research questions, which will be verified using the SMC, have been defined:

1) Is the controller switching state distribution uniform? Does it differ depending on the grid distortion?
2) What is the average root mean square difference ($RMSD$) of the output current for various harmonic grid distortions and grid sag types?
3) How do the parameter uncertainties (mismatched parameters in the prediction model and physical system) affect the performance? Does it differ if all system variables are measured or if some are estimated?
4) Is the device stress distribution even? How is it affected by harmonic grid distortion? What is the influence of the cost function design?

Due to the fact that the FS-MPC algorithm has a variable switching frequency, device stress distribution cannot be easily performed using loss equations. Different grid conditions paired with different weighting factors used in the algorithm will provide different stress distributions. Methods that explore a single run of the system will be unable to cover all the converter operating points or easily gain insight into the statistical evidence of the system performance.

The main contributions of this research paper are:

1) The proposal of a novel modular modelling approach with simple building blocks for applying the statistical verifi-

cation of grid connected FS-MPC controlled converters. This simplifies and speeds up the creation of new models.
2) The verification of the FS-MPC algorithm under different harmonic distortion levels and voltage sags to evaluate its performance. Critical operating conditions can be found and their impact on the performance can be reduced.
3) The evaluation of converter switching state distribution and device utilization to estimate the stress under different operating conditions. The control parameters can then be tuned for the best performance/lifetime ratio.
4) The evaluation of robustness under parameter uncertainties to estimate the level of performance degradation for a different number of measurement sensors. It will reveal if their number can be reduced.

The rest of the paper is structured as follows. Section II provides some general information about the system model. The novel modular modelling in UPPAAL SMC is presented in Section III. Section IV shows the results of statistical model checking for the defined research questions. Experimental results for the verified control algorithm are shown in Section V. Finally, Section VI summarizes and concludes the article.

II. SYSTEM MODEL

A. Electrical model

A matrix converter can be described as a PES with a complex structure and with a large number of power electronic devices, responsible for direct AC/AC conversion [26]. The structure of the converter is a matrix of bidirectional semiconductor devices directly switching the three-phase power grid to the inductive load as shown in Fig. 1. The performance is influenced by both the control strategy and the distortion of the power grid. It is possible to independently control the output currents and the input power factor. The matrix converter is connected to a three-phase voltage source through a low-pass input filter, where the cut-off frequency depends on the filter parameters. The main purposes of using this filter is the elimination of high-frequency harmonics in the input currents and the elimination of overvoltages which occur due to the fast commutation of large currents and the short-circuits on the impedance of the supply network.

B. Control algorithm

As mentioned in the introduction the matrix converter will be operated using the FS-MPC algorithm. In the FS-MPC algorithm the control actions are based on predicted values of the system variables. The predictions are calculated for all allowed converter operation states (27 in total) using the system model and afterwards evaluated in the cost function. Next, the converter state that will provide the minimum cost function value is selected among allowed converter operation states. The source filter system model can be described by the following state space equations (1) and the load model by the differential equation (2), where L_S, R_S and C_S represent the output filter inductance, resistance and capacitance, L_{Load} and R_{Load} are load inductance and resistance, respectively. The converter model is defined by (3) and (4) describing the voltage and current relationships at the output and input.

$$\begin{bmatrix} \frac{dv_{in,\ abc}}{dt} \\ \frac{di_{S,\ abc}}{dt} \end{bmatrix} = \begin{bmatrix} 0 & \frac{1}{C_S} \\ \frac{-1}{L_S} & \frac{-R_S}{L_S} \end{bmatrix} \begin{bmatrix} v_{in,\ abc} \\ i_{S,\ abc} \end{bmatrix} + + \begin{bmatrix} 0 & \frac{-1}{C_S} \\ \frac{1}{L_S} & \frac{-R_S}{L_S} \end{bmatrix} \begin{bmatrix} v_{S,\ abc} \\ i_{in,\ abc} \end{bmatrix} \quad (1)$$

$$L_{Load}\frac{di_{o,\ abc}}{dt} = v_{o,\ abc} - R_{Load}i_{o,\ abc} \quad (2)$$

$$\begin{bmatrix} u_{oa} \\ u_{ob} \\ u_{oc} \end{bmatrix} = \begin{bmatrix} s_{aA} & s_{bA} & s_{cA} \\ s_{aB} & s_{bB} & s_{cB} \\ s_{aC} & s_{bC} & s_{cC} \end{bmatrix} \begin{bmatrix} u_{in\ a} \\ u_{in\ b} \\ u_{in\ c} \end{bmatrix} \quad (3)$$

$$\begin{bmatrix} i_{in\ a} \\ i_{in\ b} \\ i_{in\ c} \end{bmatrix} = \begin{bmatrix} s_{aA} & s_{aB} & s_{aC} \\ s_{bA} & s_{bB} & s_{bC} \\ s_{cA} & s_{cB} & s_{cC} \end{bmatrix} \begin{bmatrix} i_{oa} \\ i_{ob} \\ i_{oc} \end{bmatrix} \quad (4)$$

To obtain a discrete system model, the equations (1) and (2) are discretized using the forward Euler method and are used to obtain the predicted values of the signals. New measurements of signals $v_{S,\ abc}$, $i_{S,\ abc}$ and $v_{in,\ abc}$ and $i_{o,\ abc}$ are obtained for each sampling period. This version of the FS-MPC algorithm is utilizing all the available measurements. It is also possible to implement the FS-MPC algorithm without using the measurements of currents $i_{S,\ abc}$ and $i_{o,\ abc}$. These values are obtained by using a system model, thus the predicted (estimated) values $i^p_{S,\ abc}$ $i^p_{o,\ abc}$ will replace the measurements in the algorithm. Consequently, fewer A/D converters are required in the digital control system. This configuration will be referred to as reduced measurement FS-MPC.

Accurately tracking the reference output current $i^*_{o,\ abc}$ by shaping the appropriate output voltage of the converter is the main goal of the algorithm. A secondary control objective with the goal of maintaining the unity input power factor is also defined. For these purposes, the cost function is defined as:

$$g = \lambda_1 \left(|i^*_{o\alpha} - i^p_{o\alpha}| + |i^*_{o\beta} - i^p_{o\beta}| \right) + \lambda_2 |v_{S\beta} i^p_{S\alpha} - v_{S\alpha} i^p_{S\beta}| \quad (5)$$

where indices α and β denote the real and imaginary part of the respective three-phase voltages and currents, which are described in the complex reference plane, $i^p_{S,\ abc}$ and $i^p_{o,\ abc}$ are the predicted values obtained using the system model, λ_1 and λ_2 are the weighting factors. The number of weighting factor combinations should be narrowed down before SMC application, since it will require a lot of time to check all combinations. An overview of methods that can be used for selection is given in [21].

One of the metrics that will be used to evaluate the performance of the algorithm is the root mean square difference of the load current (RMSD) and the reference current, defined by the equation:

$$RMSD = \sqrt{\frac{\sum_{j=1}^{N}(i_j - i^*_j)}{N}} \quad (6)$$

where N represents the number of samples, i_j is the measured load current and i^*_j is the reference current.

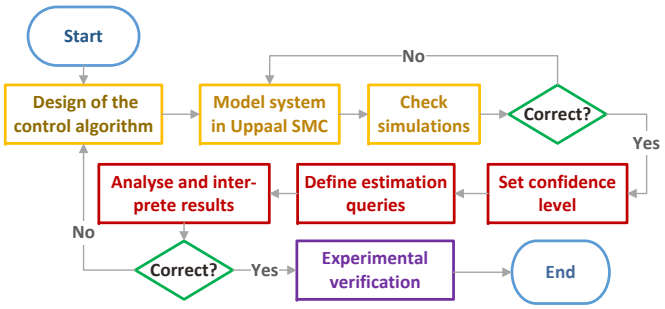

Fig. 2: The proposed process flow with statistical model checking (SMC).

III. Modular Modelling Approach

This section describes the modular approach used for modelling the power electronics components. UPPAAL SMC was used, a tool which has its origin in the non-statistical model checking tool UPPAAL, and was extended with statistical analysis in 2012 [18]. In previous papers applying UPPAAL SMC to PES [4], [19], [27] the modelling was tailored to an individual controller and obtaining results from the model. In this paper we emphasize the simplifying of the model as much as possible as well as establishing interfaces between different components. This will enable the future modelling of more complex compositions of PES using modular components.

The proposed process flow shown in Fig. 2 starts with the design of the control algorithm. The components of the PES are modelled using the TA structures in UPPAAL SMC and then connected to each other as in Fig. 3. Examples of PES components are given in Fig. 4 and Fig. 5. Then, the complete model is simulated, and the obtained waveforms are analyzed to validate the model correctness. First the confidence level is set and then the statistical validation can be performed by checking various estimation queries (for specified configurations) and analysing them. If the results of SMC are satisfying, experimental validation can be performed. Otherwise, it is necessary to go back to the step of redesigning the control algorithm. Finally, experimental verification confirms the correct operation of the control algorithm.

A. Controller model

A model in UPPAAL SMC consists of *global declarations*, a set of *templates* and a *system declaration*. Due to the page limitation, the details of the complete model will not be presented in this section. However, the full model can be accessed in referenced supplementary files. The *global declarations* and other textual parts of UPPAAL SMC models are written in a subset of the programming language `C`. In our model, one model time-unit is set to be equal to one microsecond. The differential equations in the model are solved by UPPAAL SMC using the Runge-Kutta method 100 times for each model time-unit. The `clock` data-type, used for real valued variables, increases linearly if not defined to follow some other differential equation. The name `clock` is an artefact of the symbolic real-time model-checking origins of UPPAAL.

After having defined a few global constants for the system, the next step is to create data structures that can represent

```
// Wires connecting the components
wire_t source_wire, output_wire;

// Definition of one instance of the components
g1 = GridPerfect(source_wire);
c1 = MatrixController(source_wire, output_wire);

// List of system components
system g1, c1;
```

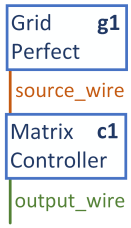

Fig. 3: System declaration of the UPPAAL SMC model.

3-phase voltages and currents. These values are represented by an array of six values of the type `clock`. Six constants are simultaneously defined `v_a`, `v_b`, `v_c`, `i_a`, `i_b`, `i_c`, each one referencing respectively the voltage `v` and current `i` of each of the wires (phases) `a`, `b` and `c`. The constants are used as static indices into the array representing a wire, thus providing an easily readable way of referring to each individual value.

The *system declaration*, shown in Fig. 3, first defines two wires, one constant specifying when the sampling starts and then two template instances. Then, the `system` is composed of two template instances `c1` and `g1`. How the wires are connected to the individual parts of the system is defined through the instantiation of the templates and shown in the small diagram in Fig. 3. The way templates and component instances relate to each other is analogous to classes and objects in object oriented programming, and thus once different types of components have been specified, they can easily be composed into more complex system setups.

The most important UPPAAL SMC components are `GridPerfect` and `MatrixController` as shown in Fig. 4. `GridPerfect` is a simple template with just one location and three differential equations that describe the way in which the grid power evolves over time. `MatrixController` has only two locations, but is much more complex. The initial location, `Init`, is also committed, marked with a "c", which indicates that no other action can happen before this location is left. This means that all the assignments on the edge leading to the `Operating` location will take effect before anything else in the model. The variables `sample` and `switching` are of the special type *clock*. As long as the automaton stays in the `Operating` location, the values of the clocks increase at the same rate. The invariants $sample <= 25.0$ and $switching <= 25.0$ define the maximum time that the automaton can stay in that location after the last reset, which occurs when taking one of the two outgoing edges. The two outgoing edges handle respectively the measurements of voltage and current as well as the switching operation. The complete behaviour of the measurements can be seen from Fig. 4, while the complexity of the switching is hidden away in three function calls: `calc_cost()`, `getCon()` and `setSwitches()`. These functions can be found in the supplementary files. The largest part of Fig. 4 shows the differential equations that describe the physics of the matrix converter. The behaviour of the converter is fully deterministic, so all the stochastic behaviour is introduced in the power grid model.

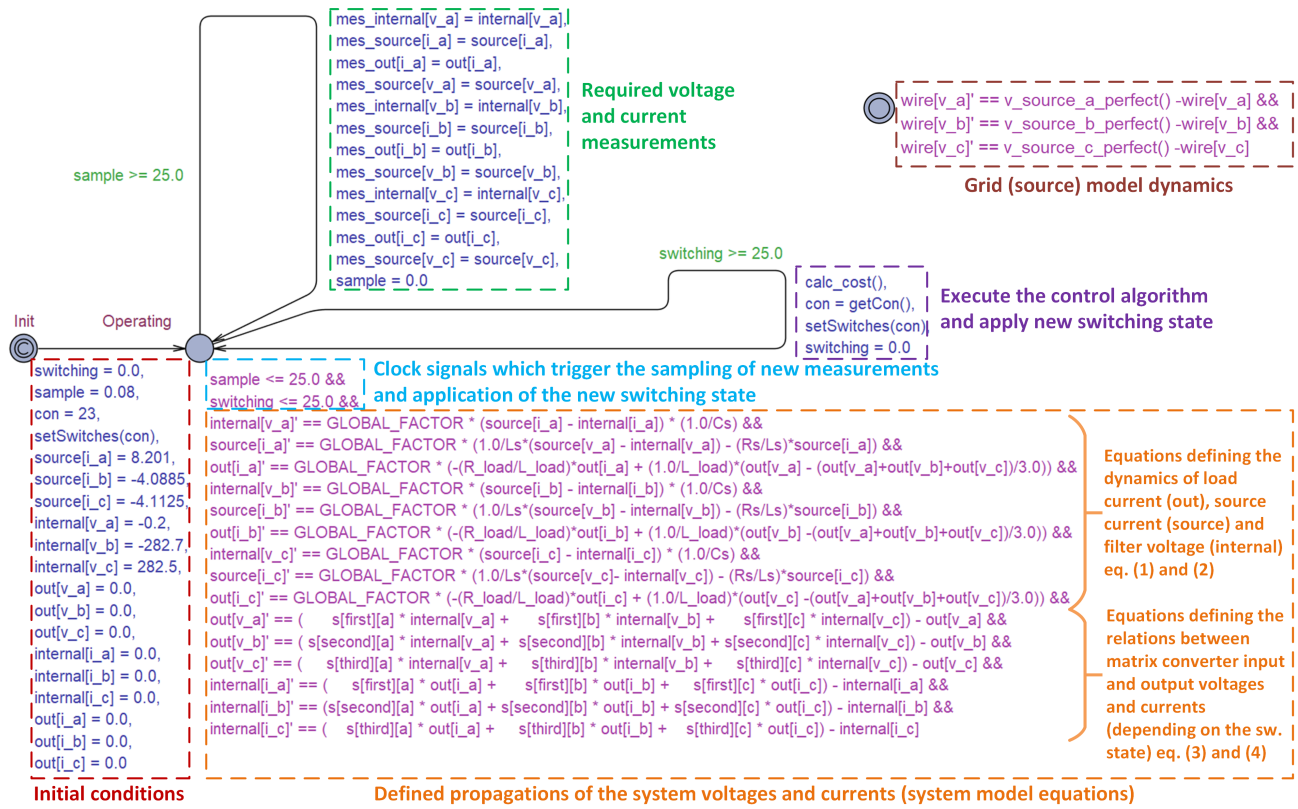

Fig. 4: Model of the matrix controller implemented in UPPAAL SMC.

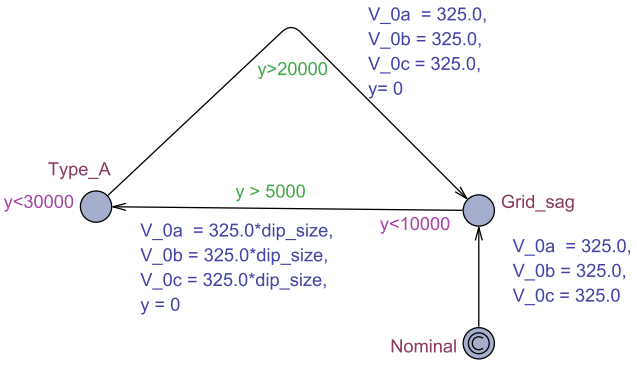

Fig. 5: Model of grid sag type A in UPPAAL SMC, V_{0a}, V_{0b}, V_{0c} are the amplitudes of the grid voltage, y is the local clock defining the voltage sag location and duration.

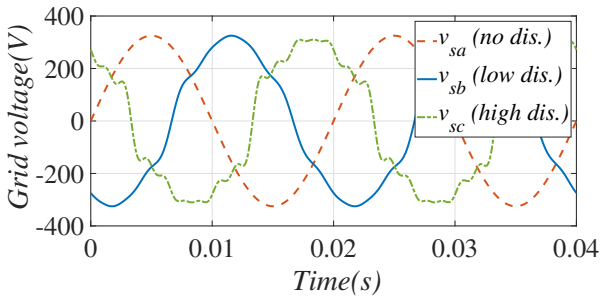

Fig. 6: Grid voltage waveforms: no distortion (no dis.), low distortion (low dis., compatibility level), high distortion (high dis., immunity level).

B. Grid model

As mentioned in the introduction, to assess the performance of the algorithm, a stochastic grid model will be used. Three levels of grid distortions – no distortion, low distortion and high distortion – are modelled separately. The structure of the distortion models is the same (leading from a perfect grid into low/high distortion), the values and equations are adjusted for the particular distortion. The low distortion grid corresponds to the compatibility level of harmonics defined by the IEC 61000-2-4 [28] and the high distortion grid corresponds to the immunity level of harmonics defined by the IEC 61800-3 [29]. The grid voltage waveforms are shown in Fig. 6.

In the ABC classification seven different grid sag types are defined based on the fault type, transformer winding connection and load connection [30]. For the application presented in this paper, grid sag types - A, B and E - were selected. Appearance of the voltage sags in the electric grid is not predictable and can potentially cause many problems in the energy supply [31], [32]. There are five features that define the voltage sags in the grid model: type, duration, depth, start and location (which phases are affected). The type and the depth are modelled as deterministic parameters to correctly quantify the obtained results. The duration, start and location are stochastic. As an illustration, a model of grid sag type A in UPPAAL SMC is shown in Fig. 5. It should be noted that initially the nominal grid parameter values are used and then randomly changed to model the stochastic behaviour of the grid. In Fig. 7 the voltage waveforms during sag types A, B and E and low level of grid distortion can be observed. Grid sag type A influences all three grid phases by reducing the

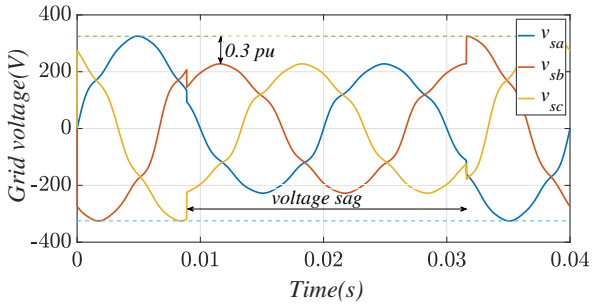

(a) Grid sag type A.

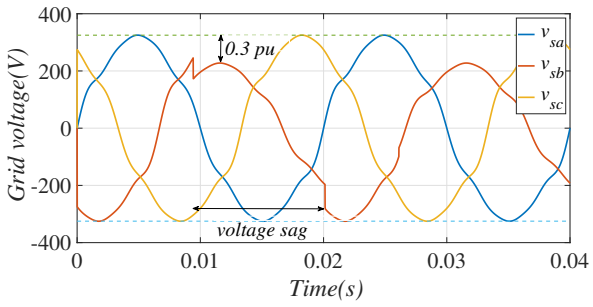

(b) Grid sag type B.

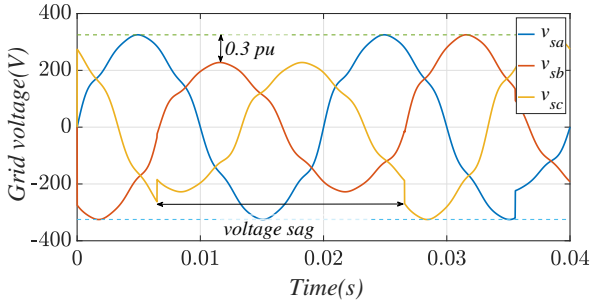

(c) Grid sag type E.

Fig. 7: Waveforms of the grid voltage sag types. Sag duration and location selected randomly in each simulation run.

voltage amplitude for a certain period. On the other hand, sag type B, influences only one phase, which is selected randomly in the model. Finally, sag type E will influence two phases, which are again chosen randomly, i.e., during one simulation all phases have the same likelihood to experience a voltage sag. Thus, in each simulation run there will be a different starting time, duration, and location of the voltage sag, which fits with the unpredictability of the real-life voltage sags in electric grids. It is important that the control algorithm can maintain a stable response in all these situations and that we identify in which conditions the performance will degrade and to what extent.

IV. Results of Statistical Model Checking

To answer the research question defined in the introduction, SMC was performed on a matrix converter model using the Uppaal SMC toolbox [33]. Probability estimation and value estimation queries have been defined to evaluate the particular aspects of functionality. Probability estimation queries return the probability of a path expression being true given that the predicate in probability brackets is true, e.g., probability that within the 44 000 time units the value of $Rmsd.c$ will be greater than 0.06 can be defined as $Pr[<= 44000](<> (Rmsd.c > 0.06))$. On the other hand, value estimation queries return the expected mean value of an expression, e.g., the maximum value of $switching[0]$ variable (counting number of switching cycles for switch $S0$ within 200 000 time units) can be defined as $E[<= 200000](max : switching[0])$.

TABLE I: Control outputs (con) and their assigned switch configurations (states) of the matrix converter.

Con	States	Con	States	Con	States
1	aaa	10	cac	19	aac
2	bbb	11	cbc	20	bbc
3	ccc	12	aba	21	bba
4	acc	13	aca	22	abc
5	bcc	14	bcb	23	acb
6	baa	15	bab	24	bac
7	caa	16	cca	25	bca
8	cbb	17	ccb	26	cab
9	abb	18	aab	27	cba

A. Controller switching state distribution

The first property that can be checked is the distribution of the controller switching states during different grid conditions. Each control output (con) has a unique switch configuration, as shown in Table I. For example: control output 27 indicates that in this switch configuration the output terminal of the matrix converter *A* is connected to the input terminal *c*, the output terminal *B* is connected to the input terminal *b* and the output terminal *C* is connected to the input terminal *a*. Using the probability estimation queries, the probabilities of each control output have been checked (within 44 000 time units which corresponds with two fundamental periods of the grid voltage and the initial transient). The results are shown in Fig. 8. For extremely low or extremely high obtained probability values, a smaller number of simulation runs was necessary (usually 29), which allowed the verification to finish within reasonable time (several minutes). For the other values between, more simulation runs have been performed, e.g., for $Con = 7$ there were between 319 and 402 simulation runs required to estimate the probability for a low grid distortion level depending on the grid sag type (the verification lasted then about seven hours). It can be observed that the probability distribution is unequal, which means that some control outputs are evidently less used than others, and so it depends on the distortion level and the grid sag type. For a case with higher distortion the rarely used control outputs of the converter were now used more often than for the low distortion. This is also the first indicator that the device stress distribution will probably also be unbalanced and that some devices will endure a higher switching stress under high distortions of the grid.

B. Performance verification

The controller performance has been evaluated for different harmonic grid distortion levels, grid sag types and voltage sags. The results are summarized in Fig. 9. Generally, it can be observed, that the particular grid sag types obtain similar results for different grid distortions, however, looking into details, some interesting observations can be made as follows.

	Low distortion			High distortion		
Con	Grid sag type A	Grid sag type B	Grid sag type E	Grid sag type A	Grid sag type B	Grid sag type E
1	[0.364,0.463]	[0.379,0.479]	[0.376,0.476]	>= 0.902	>= 0.902	>= 0.902
2-3	<= 0.098	<= 0.098	<= 0.098	<= 0.098	<= 0.098	<= 0.098
4-5	>= 0.902	>= 0.902	>= 0.902	>= 0.902	>= 0.902	>= 0.902
6	[0.261,0.361]	[0.091,0.191]	[0.244,0.343]	[0.74,0.84]	[0.817,0.917]	[0.771,0.871]
7	[0.46,0.56]	[0.681,0.781]	[0.55,0.65]	>= 0.902	>= 0.902	>= 0.902
8-13	>= 0.902	>= 0.902	>= 0.902	>= 0.902	>= 0.902	>= 0.902
14	[0.519,0.619]	[0.217,0.317]	[0.381,0.481]	>= 0.902	>= 0.902	>= 0.902
15	[0.537,0.637]	[0.65,0.75]	[0.527,0.627]	>= 0.902	>= 0.902	>= 0.902
16	[0.666,0.766]	[0.523,0.623]	[0.605,0.705]	>= 0.902	>= 0.902	>= 0.902
17	[0.065,0.165]	[0.154,0.253]	[0.143,0.243]	[0.867,0.966]	[0.888,0.987]	>= 0.902
18-23	>= 0.902	>= 0.902	>= 0.902	>= 0.902	>= 0.902	>= 0.902
24	[0.593,0.693]	[0.34,0.44]	[0.543,0.643]	>= 0.902	>= 0.902	>= 0.902
25	<= 0.098	<= 0.098	<= 0.098	<= 0.098	<= 0.098	<= 0.098
26	<= 0.098	<= 0.098	<= 0.098	[0.065,0.165]	[0.162,0.262]	[0.109,0.209]
27	[0.24,0.34]	[0.077,0.177]	[0.158,0.258]	>= 0.902	>= 0.902	>= 0.902

Fig. 8: Probabilities of different control outputs (con) of the controller for different distortion levels.

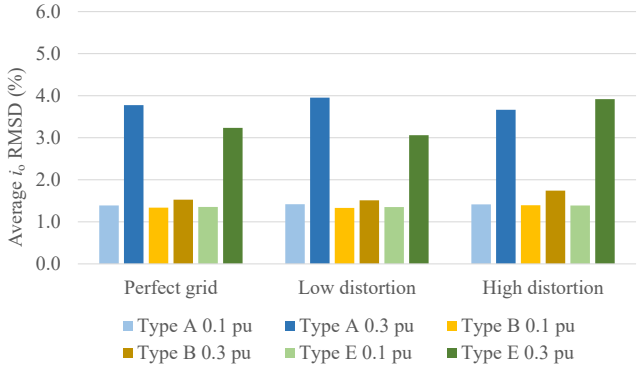

Fig. 9: Average $RMSD$ of the load current obtained for different grid level distortions and voltage sag types.

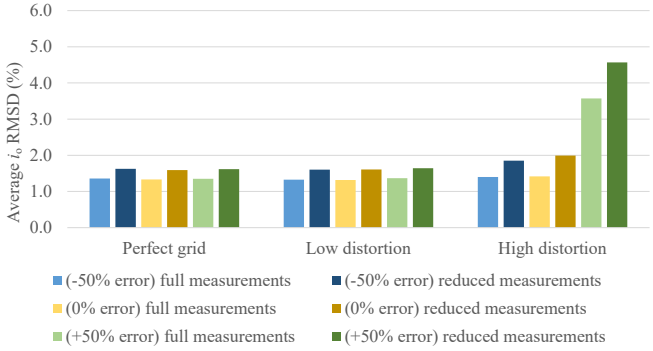

Fig. 10: Average $RMSD$ of the load current obtained for full and reduced measurements with no voltage sags, different grid level distortions and introduced parameter errors.

1) Under harmonic grid distortion: Three grid distortions have been taken into account, namely a grid without distortion, with low distortion and with high distortion. The controller performance under grid sag Type B is the least affected, obtaining similar results regardless of the level of harmonic distortion because only one phase is affected by the sag.

2) Under voltage sags: Effects of three grid sag types A, B and E shown in Fig. 7 with two different sag amplitudes have been analyzed. The voltage sags 0.1 pu and 0.3 pu correspond to the situations when the grid voltage drops to 90% and 70% of the nominal value. The controller performance under grid sag Type A and Type E shows a similar trend, i.e., the average $RMSD$ is evidently much higher for voltage sag amplitude of 0.3 pu (approx. three times bigger in comparison to obtained values for voltage sag amplitude 0.1 pu). In contrast, the controller performance under grid sag Type B seems again not to be very affected - the $RMSD$ values for voltage sags 0.1 pu and 0.3 pu are very similar, with just a slight increase for the voltage sag 0.3 pu. Therefore, it can be concluded that low amplitude voltage sags will not have a large effect on the controller performance, while high amplitude sags of Type A and E will significantly impair the controller performance and the quality of the current delivered to the load.

C. Robustness verification under parameter uncertainties

The robustness under parameter uncertainties has been evaluated for a controller, which is using all the available current and voltage measurements and for the controller, which is using a reduced number of measurements (currents $i_{S,\ abc}$ and $i_{o,\ abc}$ are estimated). The results have then been compared in order to find out if the current controller performance will degrade during grid disturbances if the system currents are estimated. To introduce the parameter mismatch in the system, the values of the LC filter (R_S, L_S and C_S) used in the converter model have been modified to equal 150% of the nominal values, and afterwards 50% of the nominal values, while the values of the filter parameters of the prediction model in the FS-MPC algorithm were kept unchanged at nominal values ($R_S = 0.02\,\Omega$, $L_S = 0.5\,mH$ and $C_S = 80\,\mu F$). Additionally, two situations have been taken into account - with no voltage sags and with grid sag Type A. All obtained results, for the three types of distortions are summarized in Fig. 10 (for no voltage sags) and in Fig. 11 (for grid sag Type A 0.1 pu).

In general, a controller with full measurements showed a better performance in comparison to the controller with reduced measurements. Nominal parameter values and the values with an introduced -50% error give similar average $RMSD$. Introducing +50% errors affects the average $RMSD$ visibly, and the obtained $RMSD$ values increase approximately three times for both types of measurements. Therefore, it can be concluded that for high distortion the controller that relies only on the prediction model and with no physical measurement of the system currents cannot provide a satisfying performance

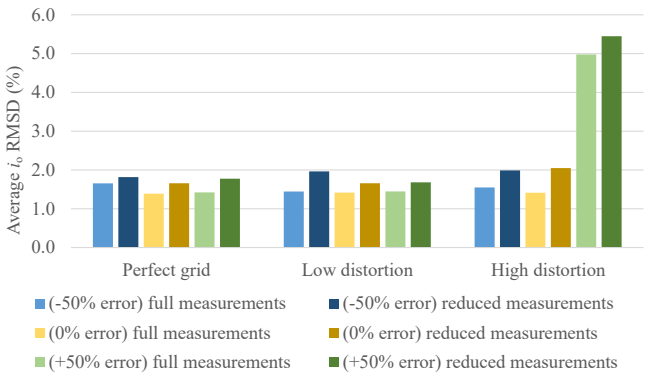

Fig. 11: Average $RMSD$ of the load current obtained for full and reduced measurements with grid sag Type A, different grid level distortions and introduced parameter errors.

for +50% errors in the prediction model parameters. However, the performance under nominal parameter values is comparable with the full measurement controller.

For both types of measurements, the average $RMSD$ for grid sag Type A is slightly higher than for no grid sags. The introduction of grid sag Type A had the highest impact on $RMSD$ for high distortion and +50% errors in prediction model parameters, where $RMSD$ was increased by 40% for a full measurement controller and 20% for a reduced measurement controller. For a low distortion and reduced measurements controller a $RMSD$ increase of 20% was also noticed.

D. Device utilization

The device utilization has been analyzed by counting the number of switching cycles for each switch during different grid distortions (no/low/high) and for the two types of cost functions. Only switching cycles with the device current above 60% of the reference value i_{ref} were taken into account, since low amplitude currents do not impose high stress on the devices. The two cost functions have different weighting factors: first has values of weighting factor λ_2 set to 0, i.e., it is used only for current control, the second has $\lambda_2 = 0.01$, i.e., it is also using the reactive power compensation. The results are summarized in Fig. 12. Two general observations are noted: that a group of switches $S1$, $S5$ and $S9$ has to endure the highest switching stress among the devices of the matrix converter; and that the number of switching cycles is two times higher than for other switches, regarding grid distortion and weighting factor value, e.g., 1265 switching cycles for switch $S5$, compared to 586 switching cycles of switch $S4$ and 733 switching cycles of switch $S6$ (for no grid distortion and $\lambda_2 = 0.01$). The number of cycles can directly affect the device utilization, as some of the switches may degrade faster due to the large number of switching cycles.

1) Effects of the harmonic grid distortion: It can also be observed that the number of switching cycles is usually the highest for the high grid distortion. However, the values for particular switches do not differ a lot, e.g, for switch $S1$: 2837/2850/3036 cycles (for no/low/high grid distortion) with $\lambda_2 = 0.00$ and 1453/1744/1727 cycles (for no/low/high grid distortion) with $\lambda_2 = 0.01$.

2) Effects of the cost function design: It can be observed that the number of switching cycles is much lower for $\lambda_2 = 0.01$ than for $\lambda_2 = 0.00$, regardless of the grid distortion (approx. half of the total numbers), e.g. for switch $S1$ (high grid distortion) there are almost 50% less switching cycles for $\lambda_2 = 0.01$ in comparison to $\lambda_2 = 0.00$. This directly influences the devices stress, as a higher number of switching cycles results in faster wear-out of the device. It also shows, that appropriately adjusting the weighting factor of the cost function can help to prolong the device lifetime, especially in the situation when the grid distortion is high.

V. Experimental verification

In the experimental verification the control algorithm has been implemented using a DSP card with Analog Devices Sharc processor (ADSP-21369) and 12 A/D converters. Dynex DIM200MBS12-A IGBT bidirectional-switch modules are used in the matrix converter prototype. The system shown in Fig. 13 is powered by programmable multi-functional power source NETWAVE 20.2, which is used to apply various types of low-frequency distortions to the three-phase supply voltage. Experimental tests were carried out using the following parameters: $L_S = 1\ mH$, $R_S = 0.01\ \Omega$, $C_S = 60\ \mu F$, $L_{Load} = 11\ mH$ and $R_{Load} = 69\ \Omega$. The FS-MPC algorithm cost function (5) was used with λ_1 = 1 and λ_2 = 0.01.

First, the experiments were performed for the case with no harmonic distortion and unbalanced source voltages. Fig. 14 shows the obtained waveforms of the source voltage and current waveforms for one phase, when a low voltage dip was applied to all three phases as follows: $U_{Sa} = 100\%$, $U_{Sb} = 90\%$, $U_{Sc} = 95\%$ of U_n where U_n is the nominal value of the voltage amplitude of fundamental harmonic. It was observed that the output currents can follow the defined set of sinusoidal reference currents under these voltage sag conditions. Next, experiments were performed to validate the transient response of the matrix converter to a three-phase symmetrical 0.1 pu voltage sag (Type A) with sinusoidal source voltages, and with injected 3rd harmonic (8% U_n) and 5th (4% U_n) harmonic. The obtained results shown in Fig. 15 confirm the correct operation of the control algorithm for low voltage sag under sinusoidal source voltages and voltage distortions. Afterwards, the experiments were repeated for 0.3 pu voltage sag as shown in Fig. 16. It has been observed that in all cases the converter provides a stable response, but the output currents cannot follow a defined set of sinusoidal reference currents after a voltage sag. The comparison of the reference tracking performance of the load current during nominal source voltage and 0.3 pu voltage sag is highlighted in Fig. 17, where it can be noticed how large the voltage sag impact is on the current. This validates the results from the SMC analysis presented in Fig. 9, where a large RMSD of the load current was obtained for 0.3 pu voltage sag for both no distortion and harmonic distortion in the source voltages, indicating that the current provided to the load will have deformations from a sinusoidal shape and an amplitude lower than the set reference.

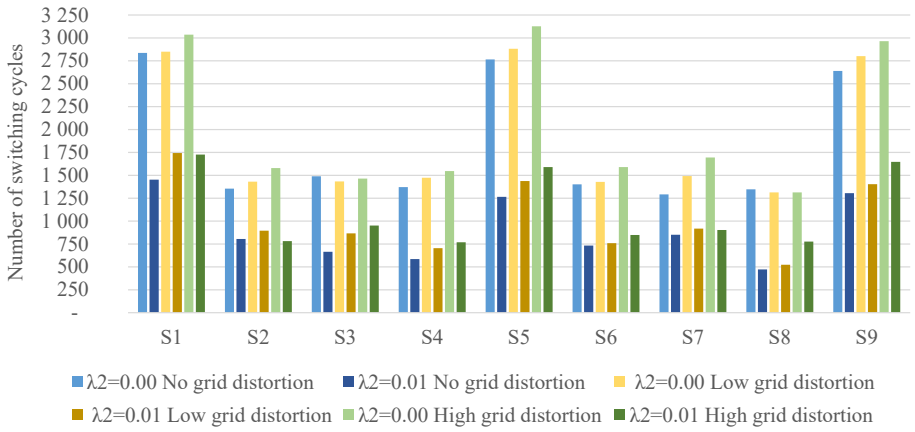

Fig. 12: Number of switching cycles for particular switches, various grid distortions and two values of weighting factor λ_2 (see Eq.(5)) in 20 fundamental cycles (0.2 s).

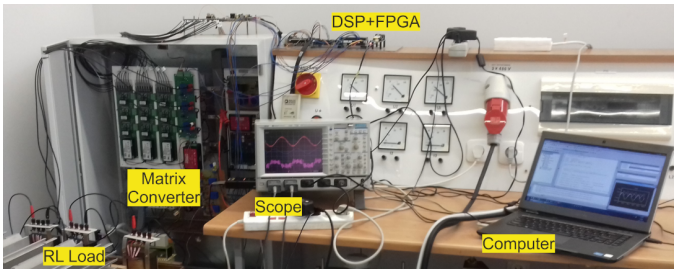

Fig. 13: Experimental setup.

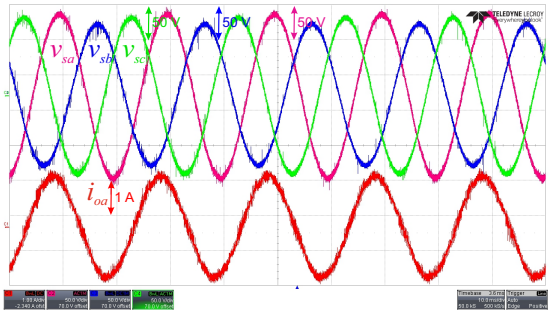

Fig. 14: Experimental results with voltage sags in the unbalanced source voltages.

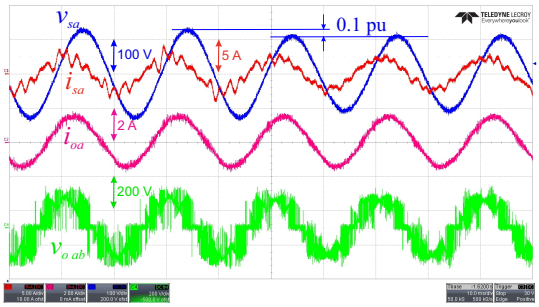

(a) Transition from nominal voltage to Type A sag (no harmonic distortion).

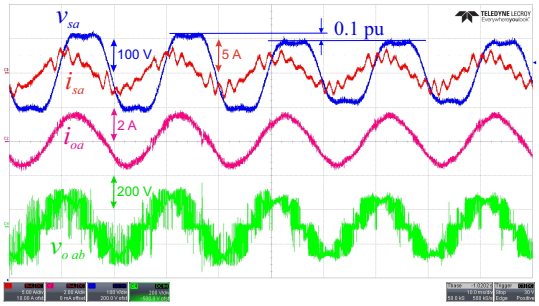

(b) Transition from nominal voltage to Type A sag (with harmonic distortion).

Fig. 15: Experimental results for the Type A 0.1 pu voltage sag with balanced and with distorted source voltages.

VI. Conclusion

In this paper a novel modelling approach for applying the statistical verification of grid connected FS-MPC controlled converters has been presented. The presented approach significantly reduces the time and effort which are required to model the dynamics of the PES. Moreover, the modelling process is similar to the traditional modelling approach of PES since the system components are now building blocks for which the user only has to define the input and output connections (wires). It has also been shown that the application of the SMC can provide information about the robustness of the control algorithm to different harmonic distortions and grid sag types. For the particular case of the matrix converter, the SMC results showed that the controller performance is sensitive to larger voltage dips of Type A and Type E, while for low voltage dips the performance remains at a similar level. If the estimated system currents are provided to the control algorithm instead of the measured ones, under high harmonic grid distortion the system cannot provide a satisfying performance below 50% error in the prediction of the model parameters.

The effects of the harmonic grid distortion and cost function design on the stress distribution among the devices were also obtained. It was shown that higher harmonic grid distortions could result in higher wear out of devices, which can be prevented by properly adjusting the weighting factors.

References

[1] S. Vazquez, J. Rodriguez, M. Rivera, L. G. Franquelo, and M. Norambuena, "Model predictive control for power converters and drives: Advances and trends," *IEEE Trans. Ind. Electron.*, vol. 64, no. 2, pp. 935–947, Feb. 2017.

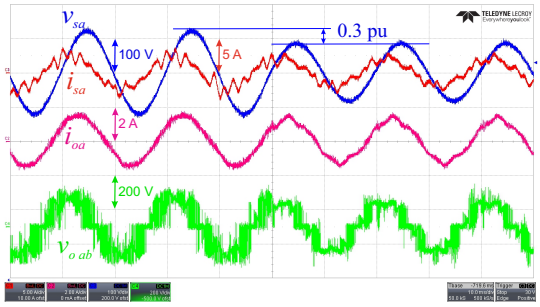

(a) Transition from nominal voltage to Type A sag (no harmonic distortion).

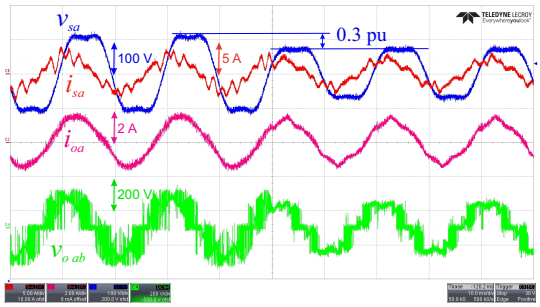

(b) Transition from nominal voltage to Type A sag (with harmonic distortion).

Fig. 16: Experimental results for the Type A 0.3 pu voltage sag with balanced and with distorted source voltages.

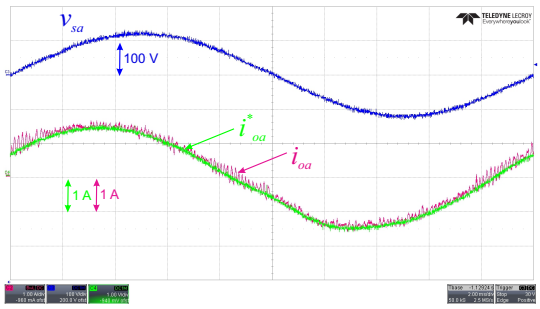

(a) Nominal source voltage.

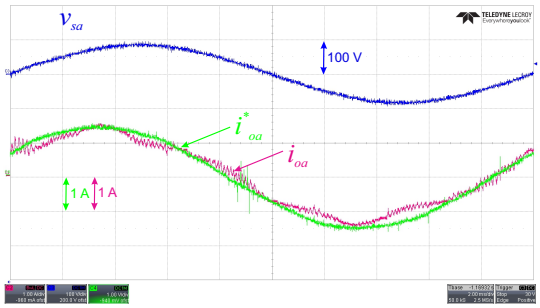

(b) 0.3 pu voltage sag.

Fig. 17: Comparison of reference i^*_{oa} and measured output current i_{oa} during 0.3 pu voltage sag and balanced source voltages.

[2] P. Karamanakos, E. Liegmann, T. Geyer, and R. Kennel, "Model predictive control of power electronic systems: Methods, results, and challenges," *IEEE Open Jour. of Ind. Appl.*, vol. 1, pp. 95–114, 2020.

[3] S. Vazquez et al., "Model predictive control: A review of its applications in power electronics," *IEEE Ind. Electron. Mag.*, vol. 8, no. 1, pp. 16–31, Mar. 2014.

[4] P. Szczesniak, I. Grobelna, M. Novak, and U. Nyman, "Overview of control algorithm verification methods in power electronics systems," *Energies*, vol. 14, no. 14, 2021.

[5] E. M. Clarke Jr, O. Grumberg, D. Kroening, D. Peled, and H. Veith, *Model checking*. MIT Press, 2018.

[6] R. Wisniewski, G. Bazydlo, P. Szczesniak, I. Grobelna, and M. Wojnakowski, "Design and verification of cyber-physical systems specified by petri nets-a case study of a direct matrix converter," *Mathematics*, vol. 7, DOI 10.3390/math7090812, no. 9, 2019.

[7] M. Miranda and A. Lima, "Formal verification and controller redesign of power electronic converters," in *Proc. of IEEE Int. Symp. on Ind. Electron.*, vol. 2, pp. 907–912 vol. 2, 2004.

[8] E. M. Hope, X. Jiang, and A. D. Dominguez-Garcia, "A reachability-based method for large-signal behavior verification of DC-DC converters," *IEEE Trans. Circuits and Systems*, vol. 58, DOI 10.1109/TCSI.2011.2157780, no. 12, pp. 2944–2955, 2011.

[9] O. A. Beg, H. Abbas, T. T. Johnson, and A. Davoudi, "Model validation of pwm DC-DC converters," *IEEE Trans. Ind. Electron.*, vol. 64, DOI 10.1109/TIE.2017.2688961, no. 9, pp. 7049–7059, 2017.

[10] S. Hossain, S. Dhople, and T. T. Johnson, "Reachability analysis of closed-loop switching power converters," in *Proc. of Power and Energy Conf. at Illinois (PECI)*, pp. 130–134, 2013.

[11] E. M. Clarke and P. Zuliani, "Statistical model checking for cyber-physical systems," in *Automated Technology for Verification and Analysis*, pp. 1–12. Springer Berlin Heidelberg, 2011.

[12] G. Agha and K. Palmskog, "A survey of statistical model checking," *ACM Trans. Model. Comput. Simul.*, vol. 28, no. 1, Jan. 2018.

[13] A. Donzé, "Breach, a toolbox for verification and parameter synthesis of hybrid systems," in *Computer Aided Verification*, T. Touili, B. Cook, and P. Jackson, Eds., pp. 167–170. Springer Berlin Heidelberg, 2010.

[14] Y. Annpureddy, C. Liu, G. Fainekos, and S. Sankaranarayanan, "S-taliro: A tool for temporal logic falsification for hybrid systems," in *Tools and Alg. for the Construction and Analy. of Systems*, pp. 254–257. Springer Berlin Heidelberg, 2011.

[15] A. Legay and L.-M. Traonouez, "Statistical model checking of simulink models with plasma lab," in *Int. Workshop on Formal Techniques for Safety-Critical Systems*, pp. 259–264. Springer, 2015.

[16] C. Menghi, E. Viganò, D. Bianculli, and L. C. Briand, "Theodore: a trace checker for cps properties," in *IEEE/ACM 43rd Int. Conf. on Software Engineering*, pp. 183–184, 2021.

[17] M. Novak, U. M. Nyman, T. Dragicevic, and F. Blaabjerg, "Statistical model checking for finite-set model predictive control converters: A tutorial on modeling and performance verification," *IEEE Ind. Electron. Mag.*, vol. 13, DOI 10.1109/MIE.2019.2916232, no. 3, pp. 6–15, 2019.

[18] P. Bulychev, A. David, K. G. Larsen, M. Mikucionis, D. Bogsted Poulsen, A. Legay, and Z. Wang, "Uppaal-smc: Statistical model checking for priced timed automata," *Electron. Proc. Theor. Comput. Sci.*, vol. 85, DOI 10.4204/eptcs.85.1, pp. 1–16, Jul. 2012.

[19] M. Novak, U. M. Nyman, T. Dragicevic, and F. Blaabjerg, "Analytical design and performance validation of finite set MPC regulated power converters," *IEEE Trans. Ind. Electron.*, vol. 66, DOI 10.1109/TIE.2018.2838073, no. 3, pp. 2004–2014, 2019.

[20] S. Boyd, C. Baratt, and S. Norman, "Linear controller design: limits of performance via convex optimization," *Proc. IEEE*, vol. 78, DOI 10.1109/5.52229, no. 3, pp. 529–574, 1990.

[21] P. Karamanakos and T. Geyer, "Guidelines for the design of finite control set model predictive controllers," *IEEE Trans. Power Electron.*, vol. 35, DOI 10.1109/TPEL.2019.2954357, no. 7, pp. 7434–7450, 2020.

[22] P. Falkowski and A. Sikorski, "Finite control set model predictive control for grid connected AC-DC converters with LCL filter," *IEEE Trans. Ind. Electron.*, vol. 65, no. 4, pp. 2844–2852, 2018.

[23] F. Wang, H. Xie, Q. Chen, S. A. Davari, J. RodrÃguez, and R. Kennel, "Parallel predictive torque control for induction machines without weighting factors," *IEEE Trans. Power Electron.*, vol. 35, DOI 10.1109/TPEL.2019.2922312, no. 2, pp. 1779–1788, 2020.

[24] J. Rodriguez, M. Rivera, J. W. Kolar, and P. W. Wheeler, "A review of control and modulation methods for matrix converters," *IEEE Trans. Ind. Electron.*, vol. 59, no. 1, pp. 58–70, 2012.

[25] G. I. Rivas-Martinez, J. Rodas, and J. D. Gandoy, "Statistical tools to evaluate the performance of current control strategies of power converters and drives," *IEEE Trans. Instrumentation and Meas.*, vol. 70, DOI 10.1109/TIM.2021.3064807, pp. 1–11, 2021.

[26] L. Empringham, J. W. Kolar, J. Rodriguez, P. W. Wheeler, and J. C. Clare, "Technological issues and industrial application of matrix converters: A review," *IEEE Trans. Ind. Electron.*, vol. 60, no. 10, pp. 4260–4271, 2013.

[27] M. Novak, U. M. Nyman, T. Dragicevic, and F. Blaabjerg, "Statistical performance verification of FCS-MPC applied to three level neutral point

clamped converter," in *Proc. of European Conf. on Power Electron. and Appl. (EPE'18 ECCE Europe)*, pp. 1–10, Sep. 2018.
[28] "Electromagnetic compatibility (EMC) - part 2-4: Environment - compatibility levels in industrial plants for low-frequency conducted disturbances," *IEC 61000-2-4*, pp. 1–75, Jun. 2002.
[29] "Adjustable speed electrical power drive systems - part 3: EMC requirements and specific test methods," *IEC 61800-3*, pp. 1–386, Feb. 2017.
[30] M. H. Bollen, *Understanding Power Quality Problems: Voltage Sags and Interruptions*. Wiley-IEEE Press, 1999.
[31] F. Iov, A. Hansen, P. Sørensen, and N. Cutululis, *Mapping of grid faults and grid codes*. Danmarks Tekniske Universitet, Risø Nationallaboratoriet for Bæredygtig Energi, 2007.
[32] H. Yang and et al., "Cause, classification of voltage sag, and voltage sag emulators and applications: A comprehensive overview," *IEEE Access*, 2020.
[33] A. David, K. G. Larsen, A. Legay, M. Mikucionis, and D. B. Poulsen, "Uppaal smc tutorial," *Int. J. Softw. Tools Technol. Transf.*, vol. 17, no. 4, pp. 397–415, Aug. 2015.

M. Novak (Member, IEEE) received the M.Sc. degree in Electrical Engineering and Information Technology from Zagreb University, Croatia, in 2014 and the Ph.D degree in Electrical Engineering from Aalborg University, Denmark, in 2020. She is currently working as a postdoctoral researcher at AAU Energy, Aalborg University, Denmark.

Her research interests include model predictive control, multilevel converters, deep learning, statistical model checking, reliability of power electronic systems and renewable energy systems. Dr. Novak is the recipient of EPE Outstanding Young EPE Member Award for the year 2019 and 2nd price winner of 2021 IEEE-IES Student and Young Professional Competition.

I. Grobelna (Member, IEEE) received the M.Sc. and Ph.D. degrees in computer science from the University of Zielona Góra, Poland, in 2007 and 2012, respectively. She is currently an Assistant Professor with the Institute of Automatic Control, Electronics and Electrical Engineering, University of Zielona Góra.

She has authored three books and co-authored over 60 scientific papers. Her current research interests include design, specification and verification of automation control systems, focusing especially on model checking.

U. Nyman is an Associate Professor at the Department of Computer Science at Aalborg University. He did his PhD Thesis on the topic of Modal Transition Systems as the Basis for Interface Theories and Product Lines under the supervision of Professor Kim G. Larsen.

His research interests lies within formal methods such as: Interface Theories, Model Checking, Compositional Verification and Software Verification. Since then he has worked with applying formal methods to different application domains. This includes model based schedulability analysis of embedded systems and statistical model checking of power electronics systems.

P. Szczesniak (Senior Member, IEEE) received the M.Sc. and Ph.D. degrees in electrical engineering from the University of Zielona Góra in 2004 and 2010, respectively. He is currently an Associate Professor with the Institute of Automatic Control, Electronics and Electrical Engineering, University of Zielona Gora.

His research interests include ac-ac converters without dc energy storage, low voltage energy storage systems and energy management in buildings.

F. Blaabjerg (Fellow Member, IEEE) received the Ph.D. degree in electrical engineering from the Aalborg University, Aalborg, Denmark, in 1995. He was with the ABB-Scandia, Randers, Denmark, from 1987 to 1988. He became an Assistant Professor in 1992, an Associate Professor in 1996, and a Full Professor of power electronics and drives in 1998 at AAU Energy. From 2017 he became a Villum Investigator. He is honoris causa at University Politehnica Timisoara (UPT), Romania in 2017 and Tallinn Technical University (TTU), Estonia in 2018.

His current research interests include power electronics and its applications such as in wind turbines, PV systems, reliability, harmonics and adjustable speed drives. He has published more than 600 journal papers in the fields of power electronics and its applications. He is the co-author of four monographs and editor of ten books in power electronics and its applications.

He has received 38 IEEE Prize Paper Awards, the IEEE PELS Distinguished Service Award in 2009, the EPE-PEMC Council Award in 2010, the IEEE William E. Newell Power Electronics Award 2014, the Villum Kann Rasmussen Research Award 2014, the Global Energy Prize in 2019 and the 2020 IEEE Edison Medal. He was the Editor-in-Chief of the IEEE TRANSACTIONS ON POWER ELECTRONICS from 2006 to 2012. He has been Distinguished Lecturer for the IEEE Power Electronics Society from 2005 to 2007 and for the IEEE Industry Applications Society from 2010 to 2011 as well as 2017 to 2018. In 2019-2020 he served as a President of IEEE Power Electronics Society. He has been Vice-President of the Danish Academy of Technical Sciences. He is nominated in 2014-2021 by Thomson Reuters to be between the most 250 cited researchers in Engineering in the world.